CHAPTER 2

MD SIMULATIONS OF KRYTOX-SILICA COMPOSITE IN NAFION MEMBRANE FOR FUEL CELL APPLICATION AT HIGH TEMPERATURE

2.1 Introduction

Nafion, a well-known polymer electrolyte fuel cell membrane produced by DuPont, is a tetrafluorethylene sulfonic acid copolymer that has a high melting point and glass transition temperature [1,2]. Its conductivity depends on the number of water molecules per sulfonic group (nH_2O/SO_3H) [3,4]. Two principal Nafion components are the main chain, consisting of tetrafluoroethylene units similar to Teflon, and the side chain which is hydrophilic ($CF_3OCF_2CF(CF_3)OCF_2CF_2SO_3H$). The hydrophilic part is made up of randomly attached long pendant side chains terminating with a sulfonic acid group. This part is important for proton diffusion and fuel cell efficiency [5-7]. The side chain molecules tend to cluster within the overall structure of the material [8-10]. One of the major problems with PEMFC is the dehydration effect at high temperatures, which leads to lower proton transfer efficiency [3,4]. In modification of polymer electrolyte fuel cell membranes to improve their efficiency at high operating temperatures ($\geq$80 ºC), composite materials such as inorganic silica are used [11-15]. Previous studies have shown that the hybrid membrane of silica composite in organic polymer membranes such as polyethylene (PEO), polypropylene oxide (PPO) and

polytetramethylene oxide (PTMO) were thermally stable at higher temperatures and had higher conductivities [11]. However, these materials would be rapidly degraded in real fuel cells by radicals from peroxide decomposition because of the presence of aliphatic hydrogens. Therefore, silica composite material should be a candidate for the modification of Nafion as well.

The study by Chirachanchai *et al*. [13,14] at the Petroleum and Petrochemical College of Chulalongkorn University used a homogeneous carboxylic acid terminated perfluoropolyether which is similar structure to Nafion hybrid with silica in Nafion (Krytox-Silica-Nafion) membrane for proton conductivity improvement. However, the aliphatic hydrogens in the Krytox-Silica structure are susceptible to degradation by radicals generated from the decomposition of peroxide in real fuel cells. Some report has been shown that the water retention and degradation temperatures were increased when the Krytox-Silica content was increased. The continuous impedance responses indicated that the bulk Nafion phase was rarely interrupted by the silica inorganic phase. The proton conductivity of pure Nafion and Nafion modified with Krytox-Silica indicated that water retention and the degradation temperature of the membrane were increased when the Krytox-Silica content was increased. When the amount of Krytox-Silica was as high as 5 %wt, the proton conductive studies under ambient conditions showed that the composite membranes maintained their conductivity at temperature up to 130 °C, better than for Nafion alone and when using other percentages of Krytox-Silica in Nafion.

In this study, we examined the microscopic properties of Krytox-Silica-Nafion polymer composite and pure Nafion systems using classical MD simulations. The MD simulations consisted of the numerical solutions of the classical equations of motion. The computer simulations help in understanding the properties of assemblies of molecules in terms of their structure and the microscopic interactions between them [16,17]. Two system models were generated. The first model consisted of 15 Nafion side chain anion's models, one Krytox-Silica molecule, and 15 hydronium ions. In another system, a pure Nafion was modeled without Krytox-Silica. The MD results from those systems were analyzed and compared in terms of proton transfer parameters, e.g. the diffusion coefficients of hydronium ions. This information will be helpful for understanding the microscopic phenomena in order to modify the fuel cell membrane using molecular level data.

2.2 Methodology

A homogeneous of coupling agent to incorporate Krytox onto a silica surface and blended with Nafion membrane was constructed as described in previous experimental work [13]. The content of aminosilane coupled onto silica particles was quantitatively analyzed and indicated that one-tenth of the aminosilane was successfully coupled onto the silica surface. When the Krytox-Silica was as high as 5 wt.% in Nafion membrane, the proton conductive studies in ambient condition have shown the best result. The structure of Krytox-Silica in Nafion side chain model was thus based on those results. A model of Krytox-Silica (Figure 2.1(a)) was constructed and its energy structure

minimized using semi-empirical AM1 by Spartan'04 program [18], and the charges were calculated by COMPASS force field ofthe Materials Studio 4.2 program package [19]. In the initial model of Nafion, the side chain ($CF_3OCF_2CF(CF_3)OCF_2CF_2SO_3H$) was optimized from conformation analysis from our previous work [20]. The 5% wt Krytox-Silica in Nafion composite polymer was used in the modification of polymer electrolyte fuel cell membrane to improve its efficiency at high operating temperatures. The 5% wt Krytox-Silica in Nafion side chain model system consisted of 15 Nafion side chains anions, one Krytox-Silica molecule, and 15 hydronium ions. The other system, a pure Nafion system without Krytox-Silica, was modeled as well. All structures of each model were randomly posited for simulation of small amorphous hydrophilic pore. Both models are shown in Figure 2.1(b) and 2.1(c). MD simulations were carried out in order to understand the microscopic properties of two systems, Krytox-Silica in Nafion and pure Nafion. NPT ensemble simulations were performed using the AMBER 9 program package [21-23] to archive the equilibrated density of 2 $g.cm^{-3}$. After that, the structure was solvated with 1,766 molecules of TIP3P water model [24] in a cubic cell to simulate the water content of fuel cell working system; this system was designated as 100% water molecules. We then performed NVT ensemble simulations at 298, 333, 353 and 373 K for another 500 ps under periodic boundary conditions. A cutoff distance (8 Å) was applied for the van der Waals forces. The electrostatic term was calculated with no cutoff. After a short energy minimization, the temperature of the whole system was gradually increased by heating to the target temperature for the first 60 ps, and then kept at that temperature from 60-600 ps using the Berendensen algorithm [25].

Separate scaling factors were used for the solute and the solvent. All trajectories were recorded and analyzed in detail. Similar simulations for 50%, 30%, and 20% of water molecules, the number of water are 883, 527, and 354, respectively.

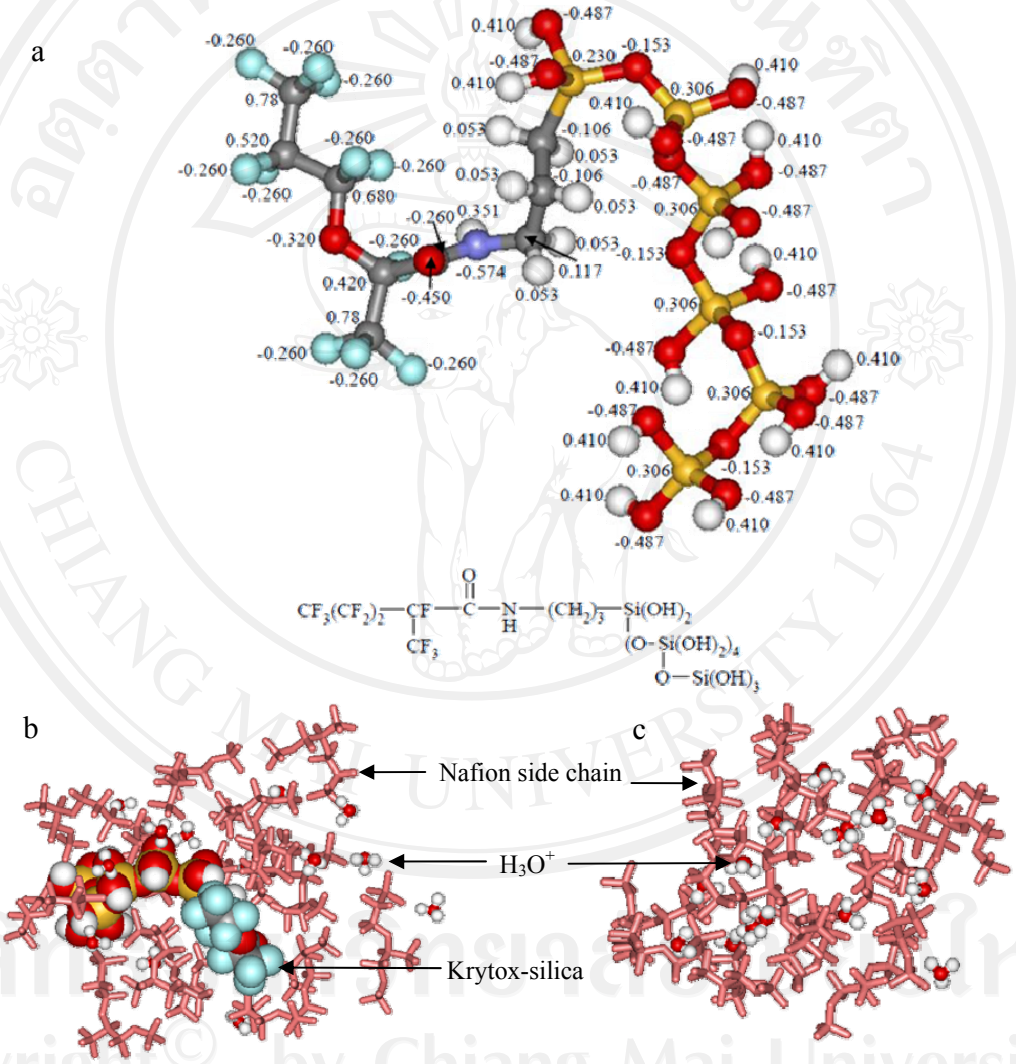

Figure 2.1 Initial structures of (a) Krytox-silica molecule and charges,
(b) 5% wt of Krytox-Silica in Nafion system, and
(c) pure Nafion system.

The efficiency of proton conduction was determined from the diffusion coefficient of hydronium ions (D). The diffusion coefficient can be calculated by the Einstein diffusion equation [26]

$$D = \frac{1}{6}\left[\frac{< [R(t) - R(0)]^2 >}{t}\right]_{t\to\infty} \quad (2.1)$$

In equation 2.1, $R(0)$ is the initial position, $R(t)$ is the position at time t and the $\langle [R(t) - R(0)]^2 \rangle$ term on the right hand is mean square displacement (MSD).

The interaction at the molecular level was investigated via the radial distribution function (RDF) (equation 2.2) [8] is the function returns the spherically averaged distribution of interatomic distance (r) between two species A and B, totaling N_A and N_B, in a volume v.

$$g_{AB}(r) = \frac{N_{AB}(r)v}{4\Pi r^2 dr N_A N_B} \quad (2.2)$$

2.3 Results and discussion

2.3.1 Effects of temperature and water content on proton conductivity

The proton conductivity averaged over 500 ps NVT simulations is shown in Table 2.1 The H_3O^+ diffusion coefficients as a function of temperature at 100% water molecules (Figure 2.2 (a)) showed that the hydronium ions' mobility was increased at high temperature. This phenomenon was consistent with the tangential direction conductivities of Nafion, of 91 and 102 mS cm^{-1} at 25 and 30 °C, respectively [3,27,28]. From the MD trajectory, the distribution of H_3O^+ around SO_3^- in terms of the RDF plot

(Figure 2.3) showed that the g(r) of H_3O^+ around SO_3^- in 5% wt of Krytox-Silica in Nafion system was higher than in the pure Nafion system at lower temperatures (298 K), whereas the opposite trend was observed at higher temperatures (373 K). From theses g(r) results, the increasing of H_3O^+ and SO_3^- interaction in composite system was decreased when the temperature increased.

Table 2.1 Diffusion coefficients of hydronium ions at different percentages of water and temperatures

% of water	**Temperature (K)**	**Diffusion coefficient ($Å^2$/ps)**	
		5% wt of Krytox-Silica in Nafion system	**Pure Nafion system**
100	333	0.26	0.40
30	353	0.39	0.26
20	373	0.26	0.24

A water content effect has been observed in several experimental studies [3, 28-30] in that the conductivity of a Nafion membrane is strongly influenced by the water content. Lower values of conductivity were observed at lower water content condition. Our simulation models assumed that at high temperatures water can evaporate; therefore, the effect of water content at the operating temperature of 353K was investigated. In our system, the water content varied from 30%, 50% and 100% relative

to the fully solvated system. The higher the percent of water molecules, the higher the diffusion coefficient of H_3O^+ (Figure 2.2(b)). The effect of the amount of water molecules on the diffusion coefficient of 5% wt of Krytox-Silica in Nafion is less than that for the pure Nafion system, especially at low water content.

Distribution of water around SO_3^- of each system is essentially the same. of experimental data [13], (e) MSD average of H_3O^+ in 5% wt of Krytox-Silica in Nafion system, and (f) MSD average of H_3O^+ in pure Nafion system. This is due to an excess of water in both systems. The distribution of water around SO_3^- in the models was shown in term of RDF of $O(SO_3^-)$-$O(H_2O)$ as shown in Figure 2.4 (top) and Table 2.2 The results showed the distribution of water around SO_3^- in Krytox-silica in Nafion system higher than pure Nafion system.

2.3.2 Comparison of proton diffusion between theoretical results and experimental data

Under the assumption that at high temperatures the water can evaporate, the percentage of water should be smaller at higher temperatures. The plot of diffusion coefficient and temperature shows a similar trend to that found from experimental measurements, reported by Chirachanchain *et al*. [13, 14] (Figure 2.2(c) and 2.2(d)).

Table 2.2 RDF of O (H_3O^+)-O(H_2O) , O(SO_3^-)-O(H_2O) and O(SO_3^-)-O(H_3O^+) and their integration number

RDF	Shell	5% of Krytox Silica in Nafion									Pure Nafion								
		333 K			353 K			373 K			333 K			353 K			373 K		
		100% water molecules			30% water molecules			20% water molecules			100% water molecules			30% water molecules			20% water molecules		
		R (Å)	g (r)	N(r)	R (Å)	g (r)	N(r)	R (Å)	g (r)	N(r)	R (Å)	g (r)	N(r)	R (Å)	g (r)	N(r)	R (Å)	g (r)	N(r)
O(H_3O^+)-O(H_2O)	1st	2.5	7.0	3.2	2.5	8.2	3.3	2.5	9.1	3.3	2.5	7.7	3.1	2.5	8.5	2.9	2.5	8.6	3.1
	2nd	4.9	1.3	16.0	4.9	1.4	15.5	4.9	1.4	15.5	4.9	1.3	16.2	4.9	1.4	14.4	4.9	1.4	14.8
O(SO_3^-)-O(H_2O)	1st	2.8	2.0	2.3	2.8	2.2	2.5	2.8	2.3	2.5	2.8	2.1	2.4	2.8	2.2	2.2	2.8	2.2	2.4
	2nd	5.2	1.2	13.6	5.2	1.3	13.7	5.2	1.3	13.7	5.2	1.2	13.2	5.2	1.3	12.5	5.2	1.3	13.3
O(SO_3^-)-O(H_3O^+)	1st	2.5	7.9	0.06	2.5	4.2	0.2	2.5	4.0	0.2	2.5	9.2	0.1	2.5	9.6	0.3	2.5	6.4	0.2
	2nd	5.0	2.6	0.6	5.0	2.2	0.9	5.0	2.2	0.9	5.0	2.8	0.8	5.0	2.9	1.2	5.0	2.4	1.1

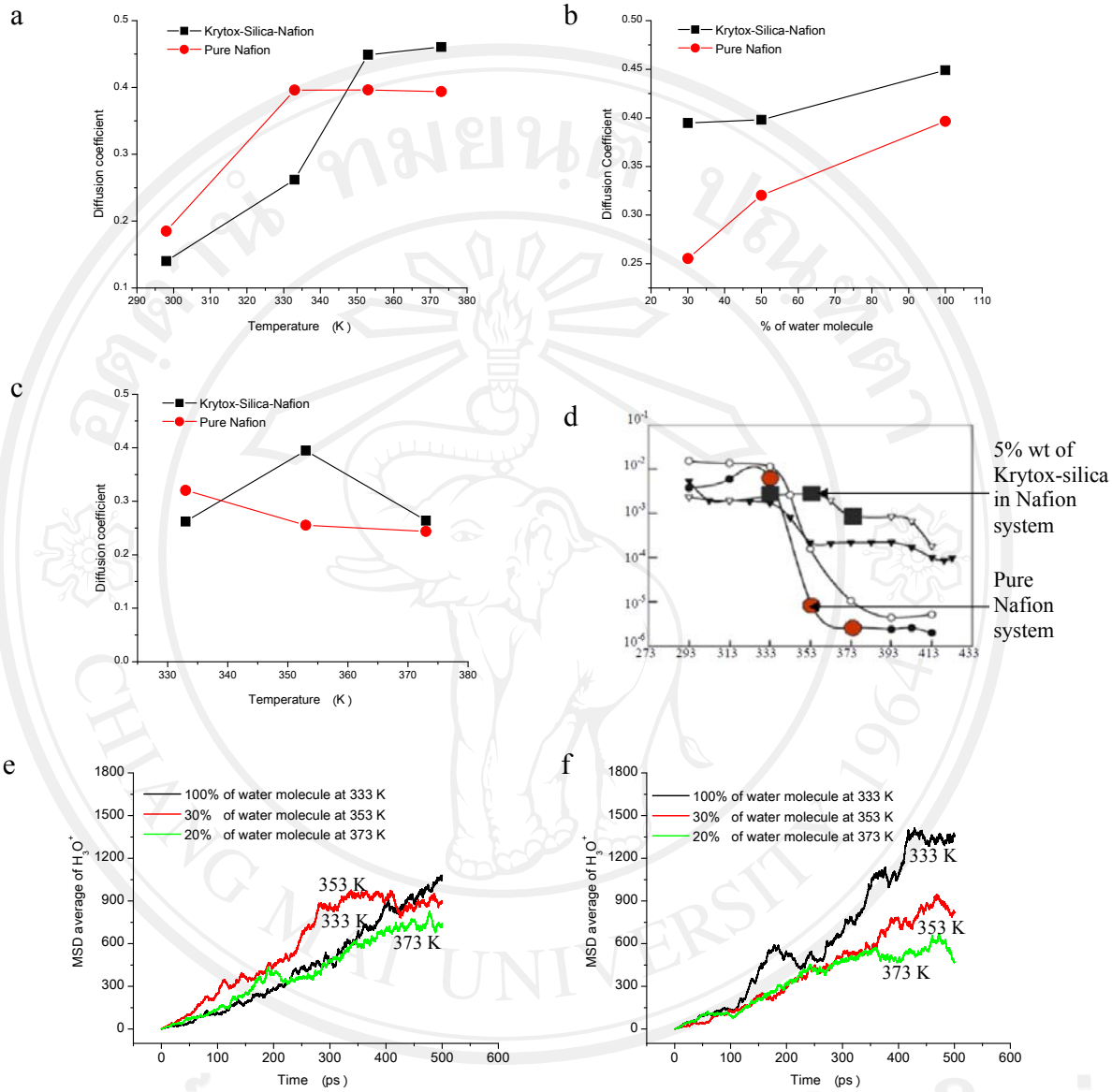

Figure 2.2 Diffusion coefficients of H_3O^+ from MD simulations: (a) variation of temperature, (b) variation of water content, (c) variation of temperature and water content, (d) proton conductivity, (e) MSD average of H_3O^+ in 5% wt of Krytox-Silica in Nafion system, and (f) MSD average of H_3O^+ in pure Nafion system

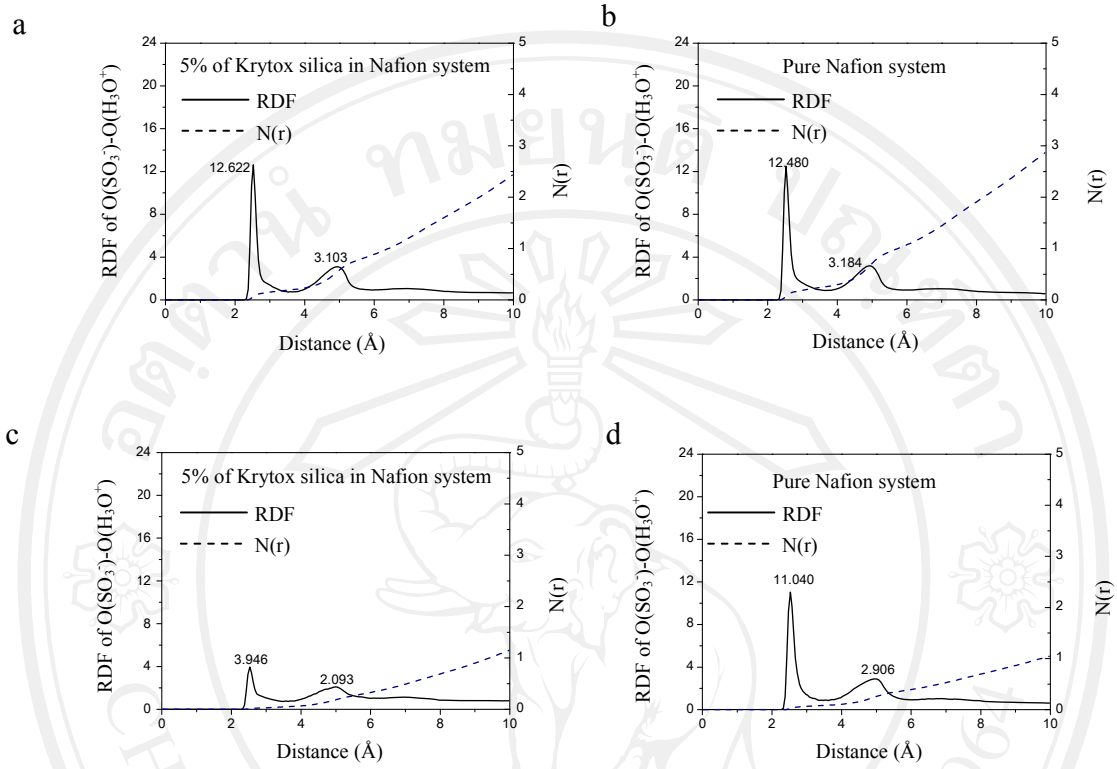

Figure 2.3 RDF graphs of $O(SO_3^-)$-$O(H_3O^+)$:

(a) 5% of Krytox silica in Nafion syste at 298 K,

(b) pure Nafion system at 298 K,

(c) 5% of Krytox silica in Nafion system 373 K,

and (c) pure Nafion system at 373 K

Many attempts studied on hydration effect on proton conduction using *ab-inito* calculation of various confined Nafion systems indicate the important role of Zundel ion in proton transfer from proton tunneling and hopping mechanism. Paddison *et.al*. [31] had used *ab initio* molecular dynamics for study of the proton transfer mechanism

between neighboring of sulfonate group. Formation of a Zundel ion ($H_5O_2^+$); a water molecule and H_3O^+ identified in a sharing of a proton transfer between neighboring of the oxygen atoms in the anionic sites with distance between oxygen atoms of water and H_3O^+ at 2.5 Å. They found that the rearrangement regarding to Zundel ion lead to an intermediate state. This drift brings thermal fluctuations which should contribute to proton conductivity. By using density functional teory, Tanimura *et.al*. also reported that the barrier energy of proton transfer using water molecule as a transporter between sulfonate ion shows lower barrier energy than direct sulfonate- sulfonate pathway [32].

In this work, the sharp peak at 2.5 Å in the RDF plot of $O(H_3O^+)$-$O(H_2O)$ for the constant 100% water model for the Krytox-Silica in Nafion system and the pure Nafion system indicated the potentially Zundel ion formation, and this complex was found related to H_3O^+ movement or proton conduction (Figure 2.4 down). This distance of $O(H_3O^+)$-$O(H_2O)$ interaction from our models corresponds to the Zundel ion of Paddison *et al.* [31]. The peak integration of the RDF plot shows that the number of water molecules around H_3O^+ in the pure Nafion system as always lower than for the Krytox-Silica in Nafion system. The results for the amount of water distributed around the hydronium ions at various water contents and temperatures are listed in Table 2.2 The interaction of SO_3^- and H_3O^+ can be investigated from the RDF of $O(SO_3^-)$-$O(H_3O^+)$ shown in Table 2.2 The distribution of H_3O^+ around SO_3^- from the peak integration of RDF plot shows that the number of H_3O^+ around SO_3^- in

both systems was not significantly different, indicating that H_3O^+ ions move between side chains only and do are stable in this interaction.

Concerning the effect of temperature, the H_3O^+ diffusion coefficients of Krytox-Silica in Nafion increased until 353 K and then kept constant, whereas the pure Nafion system had a positive slope until 333K (Figure 2.2(a)). Concerning water content (Figure 2.2(b)), the H_3O^+ diffusion coefficient of 5% wt Krytox-silica in Nafion system was constant beyond 50% water molecules, but the pure Nafion system the same coefficient was decreasing with a higher slope below that point. From results, the selected diffusion coefficients for the 5% wt Krytox-silica in Nafion system were increased from 333 K to 353 K and decreased from 353 K to 373 K as a result of the temperature and water content effects, respectively (Figure 2.2(c) and 2.2(d)). However, the diffusion coefficient of H_3O^+ in pure Nafion was mainly influenced by the water content.

2.3.3 Structural and dynamics investigation

The correlation between water content and temperature can be observed, indicating higher water content found at the lower temperature (Table 2.2) and the 5% wt of Krytox-Silica in Nafion system had higher proton conductivity at higher temperatures, as the silica can retain water in the system.

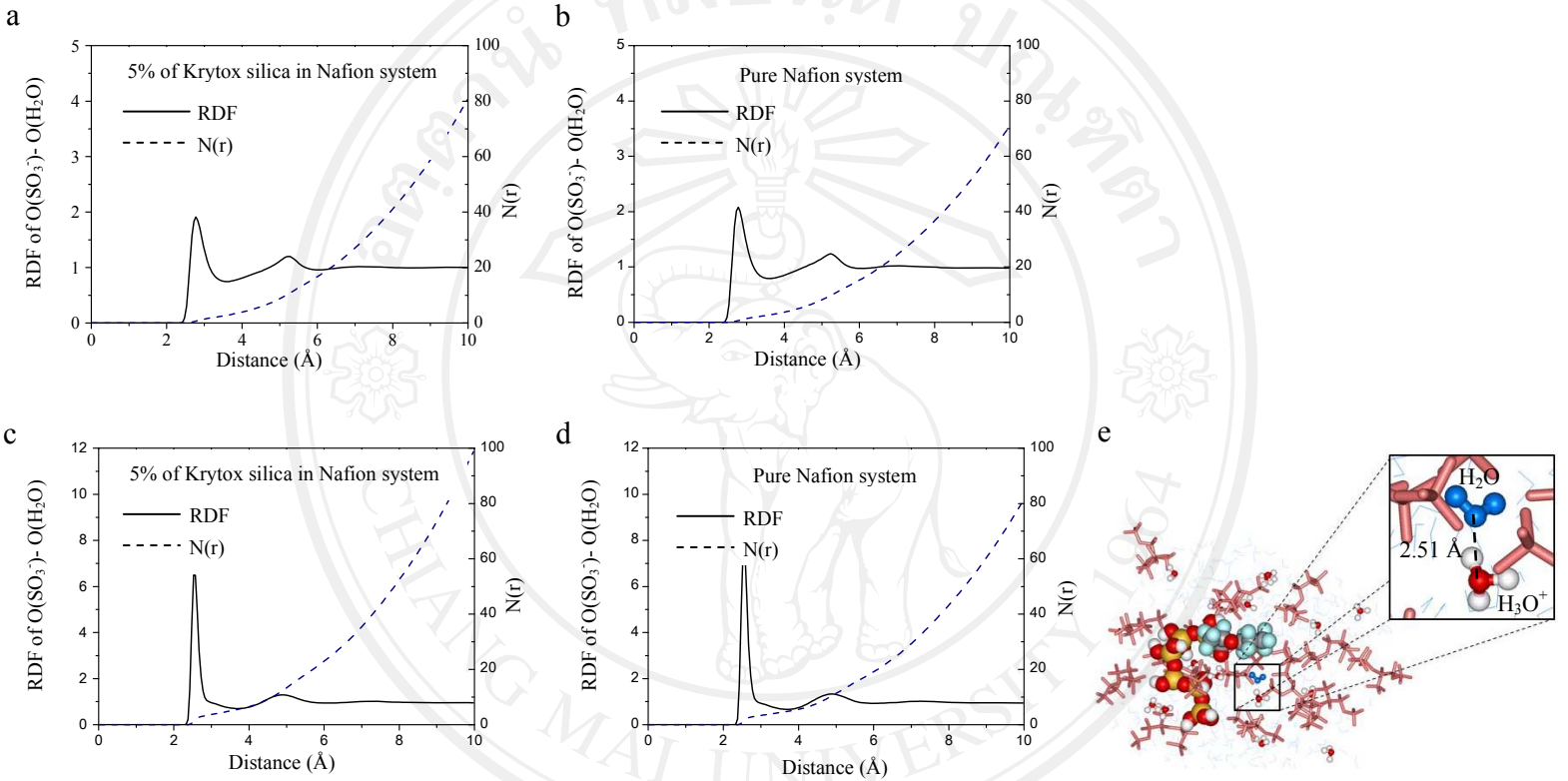

Figure 2.4 RDF graphs of $O(SO_3^-)$-$O(H_2O)$ and $O(H_3O^+)$-$O(H_2O)$: (a) RDF of $O(SO_3^-)$-$O(H_2O)$ in 5% of Krytox silica in Nafion system, (b) RDF of $O(SO_3^-)$-$O(H_2O)$ in pure Nafion system, (c) RDF of $O(H_3O^+)$-$O(H_2O)$ in 5% of Krytox silica in Nafion system, (d) RDF of $O(H_3O^+)$-$O(H_2O)$ in pure Nafion system, and (e) interaction of H_3O^+ and water molecule as act as Zundel ion like in 5% of Krytox silica in Nafion system at 500 ps

2.3.3.1 Water solvation in hydrophilic pore and water diffusion in the hydrophobic pore of Nafion

The solvation of water molecules in the hydrophilic pore can be investigated from the RDF of $O(SO_3^-)$-$O(H_2O)$ for the 100% water model at 373K, as shown in Figure 2.4 top. As a result (Table 2.2), the distribution around SO_3^- from the peak integration at 2.8 Å of the RDF shows that the number of water molecules around SO_3^- in the pure Nafion system was less than for the 5% wt Krytox-Silica in Nafion system at 353 K (30 percentage of water molecule) and 373 K (20 percentage of water molecule). Again, the number of water molecules distributed around the SO_3^- group in all systems was not significantly different, because the amounts of water per sulfonate group are sufficient for each of the systems, which used higher amounts of water than those from published experiment data.

The hydrophobic phenomena were explored by the interaction of water molecules and fluorine atoms of the Krytox component of the 5% wt Krytox-Silica in Nafion system via F(Krytox)-$O(H_2O)$ and F(Nafion)-$O(H_2O)$ RDF. The F(Krytox)-$O(H_2O)$ and F(Nafion)-$O(H_2O)$ RDF graphs are shown in Figure 2.5. There was no sharp peak at 10 Å radius. Thus, it appeared that the water molecules did not enter the non-polar component.

2.3.3.2 Hydronium ion diffusion and water absorption on the silica part of the hybrid membrane

The RDF of H(Silica)-(O(H_3O^+) was used to analyzed the interaction between H_3O^+ and Silica. The RDF graphs are shown in Figure 2.6(a). There are no sharp peaks seen in the RDFs; thus H_3O^+ did not have much interaction in the silica portion of Krytox-Silica. According to RDF analysis, from RDF between H(Silica)-(O(H_3O^+) and H(Silica)-(O(H_2O) indicated that the hydroxyl groups of silica (OH) strongly interacted with water molecules but not with H_3O^+.

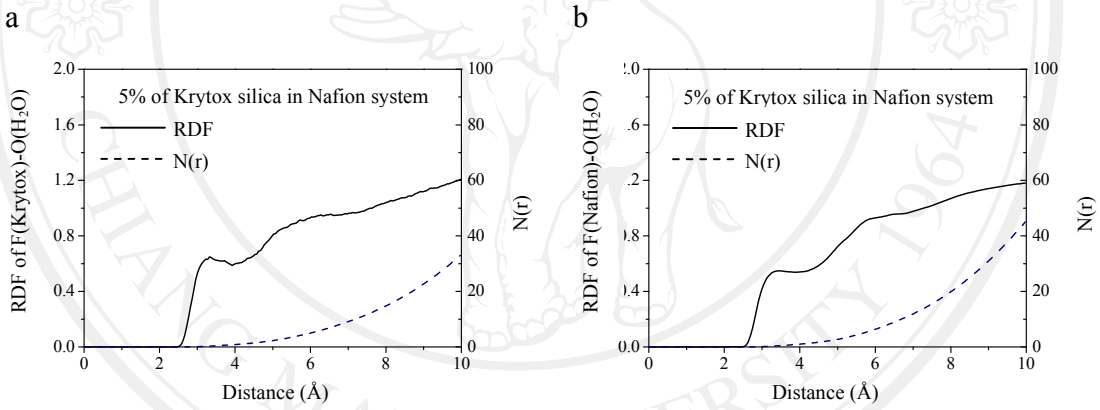

Figure 2.5 RDF graphs of the hydrophobic portion and water in 5% of Krytox silica in Nafion system: (a) RDF of F(Krytox)-O(H_2O) and (b) F(Nafion)-O(H_2O)

The interaction of water molecules and the silica component of the 5% wt Krytox-Silica in Nafion system can be investigated from the RDF (Figure 2.6(b)). A sharp peak of water distributed around the silica is seen at 1.8 Å. Almost no water molecules from the peak integration indicated were observed in the silica, which may indicate that silica did not form a strong interaction with water, and thus proton

conductivities are minimally affected effect by the 5% wt Krytox-Silica in the Nafion. Krytox-Silica material should act as a water absorbent in the hybrid polymer membrane system; this will not interrupt the proton diffusion process.

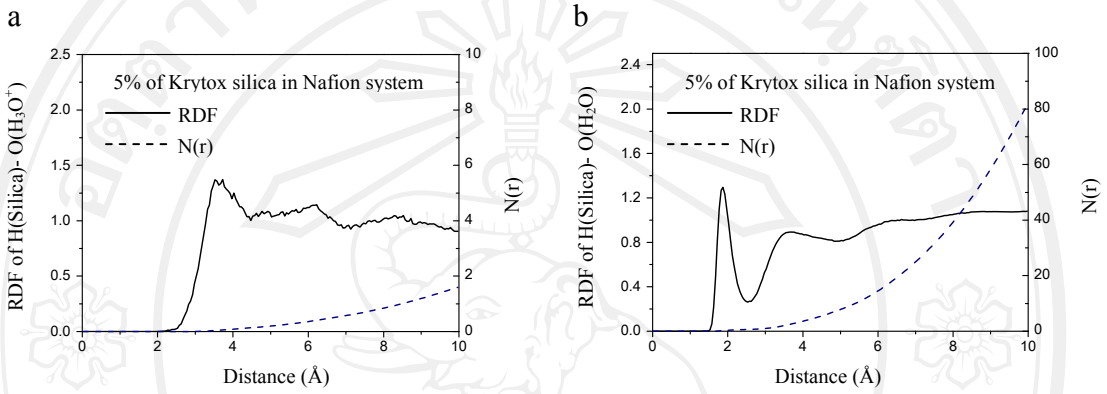

Figure 2.6 RDF graphs of (a) H(Silica)-O(H_3O^+) and (b) H(Silica)-O(H_2O)

2.4 Conclusion

MD simulations were carried out to understand the microscopic properties of 5% wt Krytox-Silica in Nafion and pure Nafion. After equilibration, the production runs were performed and stored every for subsequent analysis of hydronium ion diffusion and interatomic interactions. Further study considered the effects of temperature and water content. MD simulations at temperatures of 298, 333, 353, and 373 K with the associated water content of 1,766, 883, 527, and 354 molecules, respectively, were used and compared with published experimental data. The results were in a good agreement with experiments, and thus could be used to describe the properties of Krytox-Silica in Nafion composites at high temperatures. The effect of the amount of

water molecules on the diffusion coefficient or proton conductivity showed greater deviation between 5% wt of Krytox-Silica-Nafion composite and pure Nafion systems at lower water content (or higher temperatures) than at high water content (or lower temperatures). We observed the H_3O^+ interaction with water molecule act as Zundel ions form as shown Figure 2.4(e), which is important in the proton transfer process [20, 31, 33]. More water was distributed around SO_3^- in the composite system. Silica, as the water absorbent in the hybrid polymer membrane, did not form a strong interaction with water and H_3O^+, therefore, the proton conductivities were not much affected by adding the Krytox-Silica in the Nafion.

References

[1] Kundu, S.; Simon, L.C.; Fowler, M.; Seabra, G. *Polymer* **2005**, *46*, 11707-11715.

[2] Corti, H.R; Nores-Pondal, F.; Buera, M.P. *Journal of Power Sources* **2006**, *161*, 799-805.

[3] Silva, R.F.; De Francesco, M.; Pozio, A. *Journal of Power Sources* **2004**, *134*, 18-26.

[4] Smitha, B.; Sridhar, S.; Khan, A.A. *Journal of Membrane Science* **2005**, 259, 10-26.

[5] Zawodzinski, T. A.; Neeman, M.; Sillerud, L. O.; Gottesfeld, S. *Journal of Physical Chemistry* **1991**, *95*, 6040-6044.

[6] Sone, Y.; Ekdunge, P.; Simonsson, D.; *Journal of Electrochemical Societies* **1996,** *143*, 1254-1259.

[7] Paddison, S. J.; Zawodzinski, T A. Jr. *Solid State Ionics* **1998**, *113–115*, 333-340.

[8] Elliott, J. A.; Hanna, S.; Elliott, A. M. S.; Cooley, G. E. *Physical Chemistry Chemical Physics* **1999**, *1*, 4855-4863.

[9] Spohr, E.; Commer, P.; Kornyshev, A. A. *Journal of Physical Chemistry B* **2004**, *106*, 10560-10569.

[10] Hristov, I. H.; Paddison, S. J.; Paul, R. *Journal of Physical Chemistry B* **2008**, *112*, 2937-2949.

[11] Honma, I.; Nomurab, S.; Nakajima, H. *Journal of Membrane Science* **2001**, *185*, 83-94.

[12] Honmaa, I.; Nakajimaa, H.; Nishikawab, O.; Sugimotob, T.; Nomura, S. *Solid State Ionics* **2003**, *162– 163*, 237-245.

[13] Gosalawit, R.; Chirachanchai, S.; Manuspiya, H.; Traversa, E. *Catalysis Today* **2006**, 118, 259-265.

[14] Gosalawit, R.; Chirachanchai, S.; Shishatskiy S.; Nunes, S. P. *Solid State Ionics* **2007**, *178*, 1627-1635.

[15] Ye, G.; Hayden, C. A.; Goward, G. R. *Macromolecules* **2007,** *40,* 1529-1537.

[16] Allen, M.P.; Tildesley, D.J. "Computer Simulation of Liquids" Clarendon Press, Oxford, **1987**.

[17] Leach, A. "Molecular Modelling: Principles and Applications" 2nd ed.; Prentice Hall, **2001**.

[18] Spartan'04, Wavefunction Inc., 18401 Von Karman Avenue, Suite 370, Irvine, CA 92612.

[19] Materials Studio, Accelrys Software Inc., San Diego, CA, **2007**.

[20] Yana, J.; Lee, V.S.; Nimmanpipug, P.; Dokmaisrijan, S.; Aukkaravittayapun, S.; Vilaithong, T. *Journal of Solid Mechanics and Materials Engineering* **2007**, *1*, 556-563.

[21] Case, D.A; Darden, T.A.; Cheatham, T.E.; Simmerling, C.L.; Wang, J.; Duke, R.E.; Luo R.; Merz, K.M.; Pearlman, D.A.; Crowley, M.; Walker, R.C.; Zhang, W.; Wang, B.; Hayik, S.; Roitberg, A.; Seabra, G.; Wong, K.F.; Paesani, F.; Wu, X.; Brozell, S.; Tsui, V.; Gohlke, H.; Yang, L.; Tan, C.; Mongan, J.; Hornak, V.; Cui, G.; Beroza, P.; Mathews, D.H.; Schafmeister, C.; Ross, W.S.; Kollman, P.A. "AMBER" 9. San Francisco: University of California; **2006**.

[22] Pearlman, D.A.; Case, D.A.; Caldwell, J.W.; Ross, W.S.; Cheatham, T.E; DeBolt, S.; Ferguson, D.; Seibel, G.; Kollman, P. *Computer Physics Communications* **1995**, *91***,** 1-41.

[23] Case, D.A.; Cheatham, T.; Darden, T.; Gohlke, H.; Luo, R.; Merz, K.M.J; Onufriev, A.; Simmerling, C.; Wang, B.; Woods, R. *Journal of Computational Chemistry* **2005**, *26*, 1668-1688.

[24] Jorgensen, W.L.; Chandrasekhar, J.; Madura, J.D.; Impey, R.W.; Klein, M.L. *Journal of Chemical Physics* **1983**, *79*, 926-935.

[25] Berendsen, H.J.C.; Postma, J.P.M.; van Gunsteren, W.F.; DiNola, A.; Haak, J.R. *Journal of Compational Physics* **1984**, *81*, 3684-3690.

[26] Aida, T.; Inomata, H. *Molecular Simulation* **2004**, *30*, 407-412.

[27] Zawodzinski, T.A.; Neeman, M.; Sillerud, L.O.; Gottesfeld, S.J. *Journal of Physical Chemistry* **1991**, *95*, 6040-6044.

[28] Kolde, J.L.; Bahar, B. *Proceedings of the Fourth Grove Fuel Cell Symposium* **1995**, *September 19-22*, London, England.

[29] Iijima, M.; Sasaki, Y.; Osada, T.; Miyamoto, K.; Nagai, M. *International Journal of Thermophysics* **2006**, *27*, 1792-1802.

[30] Fontanella, J.J.; Edmondson, C.A.; Wintersgill, M.; Wu, Y.; Greenbaum, S.G. *Macromolecules* **1996,** *29*, 4944-4951.

[31] Eikerling, M.; Paddison, S.J.; Pratt, L.R.; Zawodzinski, T.A. Jr. *Chemical Physics Letters* **2003**, *368*, 108-114.

[32] Tanimura, S.; Matsuoka, T. *Journal of Polymer Science Part B: Polymer Physics* **2004**, *42*, 1905-1914.

[33] Kreuer, K.D. *Solid State Ionics* **1997**, *94*, 55-62.